Probabilistic Cellular Automata modeling of intercellular interactions in airways: complex pattern formation in patients with Chronic Obstructive Pulmonary Disease

Isabelle Dupin, Edmée Eyraud, Élise Maurat, Jean-Marc Sac-Épée, Pierre Vallois

Modeling cell interactions driving Chronic Obstructive Pulmonary Disease (COPD) via probabilistic cellular automata

Isabelle Dupin[1,2], Edmée Eyraud[1,2], Élise Maurat[1,2], Jean-Marc Sac-Épée[3] and Pierre Vallois[3]*

[1] Univ-Bordeaux, Centre de Recherche Cardio-thoracique de Bordeaux, U1045, F-33000 Bordeaux, France

[2] INSERM, Centre de Recherche Cardio-thoracique de Bordeaux, U1045, F-33000 Bordeaux, France

[3] Université de Lorraine, CNRS, Inria, IECL. F-54000 Nancy, France

*Email corresponding author : pierre.vallois@univ-lorraine.fr (Pierre Vallois)

Abstract
The chronic obstructive pulmonary disease (COPD) is a highly prevalent lung disease, in which unusual interactions between fibrocytes and CD8+ T lymphocytes in the peribronchial area could induce chronic inflammation and tissue remodeling. We considered a probabilistic cellular automata type model where the two types of cells follow simple local interaction rules taking into account cell death, proliferation, migration and infiltration. A rigorous mathematical analysis carried out within the framework of a simplified model makes it possible to estimate with precision the parameters of the model using multiscale experimental data obtained in control and disease conditions. Our model is easy to simulate. In simulations, two distinct patterns emerged, which can be analyzed quantitatively. In particular, we show that the change in fibrocyte density in the COPD condition is mainly the consequence of their infiltration into the lung during exacerbations, suggesting possible explanations for experimental observations in normal and COPD tissue. Our integrated approach combining probabilistic cellular automata type model and experimental findings will provide further insights into COPD in future studies.

Keywords :
Probabilistic Cellular Automaton, fibrocytes, lymphocytes, chronic respiratory disease, local environment, Markov process.

Fundings
This study was supported by a grant from the “Fondation Bordeaux Université”, with funding from "Assistance Ventilatoire à Domicile" (AVAD) and "Fédération Girondine de Lutte contre les Maladies Respiratoires" (FGLMR).

1 Introduction

We are particularly interested in chronic obstructive pulmonary disease (COPD), a chronic respiratory disease that affects adults over 40 years of age. The major risk factor is exposure to cigarette smoke. COPD patients often experience "exacerbations", which are periods of acute worsening of their respiratory symptoms, which play an important role in the progression of the disease. COPD is characterized by chronic bronchial inflammation of the airways and parenchyma, and airway remodeling. The lung tissue of COPD patients is infiltrated with a large amount of lymphocytes, and in particular CD8+ T cells. The density of CD8+ T cells in lung parenchyma and small airways inversely correlates with lung function [20], suggesting the implication of CD8+ T cells in deleterious COPD evolution. Changes in the structure of the tissue are also observed, such as lamina propria fibrosis of the so-called "distal" bronchi, i.e. bronchi with a lumen diameter of less than 2 mm. We have previously shown that fibrocytes, circulating cells with fibroblastic properties, were present in increased levels in the blood of COPD patients at the time of an exacerbation ([4]) and increased densities in the bronchi of COPD patients [4].
The development of the disease could be the result of complex interactions between immune cells (including CD8+ T cells) and structural cells (including fibroblast-like cells). In particular, it was recently shown that fibrocytes promote the proliferation of CD8+ T cells [1], suggesting that the interplay between these two cell types could play a role in COPD onset and evolution. Nevertheless, we are very far from understanding how the system works at the population and tissue level. Moreover, it is also difficult to know how and to what extent the disease disrupts this system.
Our working hypothesis is the following : modifications of the local interactions between fibrocytes and CD8+ T cells are the trigger to alter spatial distribution of cells, corresponding to the pathological state. This hypothesis is very difficult to test experimentally. The selected mathematical model and especially the simulations associated with it should allow to show how modications of the local interaction rules lead to two distributions of fibrocytes and CD8+ T cells, that differ according to whether the subject considered is healthy or sick. This difference could be evidenced by quantifying fibrocyte and CD8+ T cell densities. In the absence of a real understanding of the interactions between CD8+ T cells and fibrocytes, we will assume them to be random.
Two-population mathematical models include deterministic models, which classically rely on predator–prey formulation. This is suitable to analyse tumor growth [2], but may not apply to model cell interaction in peribronchial area. In addition, spatial informations and the discrete nature of cells are usually lacking in those models. The individual nature of cells can be taken into account by agent-based models, which also allow to derive more easily the interaction rules from experimental data. Among agent-based models, Lattice Gas Cellular Automaton models (see Sections 5.4 and 7 in [3]) could be relevant to our needs [9] but they are mainly used to model single and collective migration. Off-lattice models, such as center-based (CBM) and deformable-cell (DCM) models, are particularly adapted for the description of tissue made of tightly adhering cells, such as epithelia and dense tumors (see Section 14.3 in Deutsch [3] a detailed list of references). This is not suitable to model the bronchial wall, which contains immune and mesenchymal cells dispersed in an extracellular connective fibrous matrix.
The framework of Probabilistic Cellular Automaton (PCA) seemed to us the most adapted to account for the local interactions of CD8+ T cells and fibrocytes, noted respectively in the following C and F. Such models have been used to study adult neurogenesis for teleost fishes

in [15] and cell differentiation in [25]. One can find in the two monographs [3] and [16] the definition of these PCAs and theoretical models as well as many examples of applications, mainly in life sciences. In contrast to "classical" PCA, which evolves synchronously in discrete time and in which the updating concerns all the cells, we have made the cells evolve one after the other as in [6] and [12]. The probability that a cell moves, dies or proliferates depends on the number of cells present in a nearby neighbourhood. We will be able to access qualitative estimates of these probabilities thanks to data from the literature and from experiments : for example, we will be able to compare the attraction/proliferation potential of CD8+ T cells purified from tissues/blood of healthy subjects or patients with COPD.
Let us briefly outline the organization of the paper. We describe in Section 2.1 the individual behavior of the C and F cells and their mutual dynamics is presented in Section 2.1.8. We show that our model is Markovian and ergodic in Section 2.2. We assume that for a healthy subject as for a sick subject, the same model applies, but with different parameters. We introduce in Section 2.3 a toy model which is obtained for some specific values of the parameters. In this setting, a rigorous mathematical analysis makes it possible to both estimate the parameters and measure the quality of these estimates (see Section 3.1).
Our model is also simulable, we present in Section 3.2 some outputs of the simulations of the toy model. The proofs of technical points are postponed in Section 5.

2 Materials and methods

The model takes into consideration cell displacement, death, proliferation and infiltration, that occurs at the stable state and during exacerbation. Indeed, C and F cells have a limited lifespan that depends on cell type and they can therefore be affected by cell death. When the cells are alive, C cells can move and proliferate, whereas F can only move. For the initial distribution, we used the mean density of non-smokers subjects, reflecting the “healthy” situation.
As stated in the introduction, in our model there are two types of subjects : those who are healthy and those who are affected by COPD. We make the assumption that these two situations can be represented by the same model, but with different parameter values. To be able to simulate the model, it is necessary to obtain numerical values for these parameters. This will be achieved through biological experiments and data from literature. We denote by λ^{ctl} (resp. λ^{COPD}) the value of the parameter λ for a healthy (resp COPD) subject.

2.1 The interaction pattern

2.1.1 Representation of the surface of interest

We consider a lattice, of dimension 103×103 where the side length of each square is $x_0 = 7\ \mu m$. Thus the surface of 49 μm^2 corresponds to an average area of a cell. Each element of the lattice is defined by 2 coordinates, where the point on the upper left (resp. lower right) corner has the coordinates $(1, 1)$ (resp. $(103, 103)$). The coordinates of the center of the lattice are $(52, 52)$. The geometry of bronchi corresponds to the transverse section of a cylinder, then we model our surface of interest, the peribronchial (also called « lamina propria »), by a crown with a "hole" in the middle. The external and internal radii of this crown are defined thanks to our measurements on the bronchial tissues :

1. the internal radius is 263 μm, which represents the length of 38 lattice sites. This has been calculated using our measurements of the corresponding disk (i.e. lumen area + epithelium surface), which is on average 216 567 μm^2.
2. The external radius is 355 μm, which represents the length of 51 lattice sites. This has been calculated using our measurements of the corresponding disk (i.e. lumen area + epithelium surface + lamina propria), which is on average 396 436 μm^2.

Then the lamina propria $\mathcal{L}$ is the set of points with coordinates (i, j) such that :

$$38 \leq \widehat{d}\big((i,j),\ (52,52)\big) \leq 51$$

where $\widehat{d}$ is the pseudo-distance : $\widehat{d}\big((i,j),\ (i',j')\big) = \lfloor \sqrt{(i-i')^2 + (j-j')^2} \rfloor$ and $\lfloor x \rfloor$ stands for the integer part of the real number x. We thus obtain a working surface containing 3 652 lattice sites (potential cells) corresponding to an area of approximately 179 000 μm^2, which is in agreement with our *in situ* measurements. In other words, the number $|\mathcal{L}|$ of elements of $\mathcal{L}$ equals 3 652. Reflecting (zero-flux) boundary conditions are imposed at the external and internal borders. On each site, there is at most one cell.
In the literature, it is described that bronchial wall thickness is increased in COPD patients, ([11], [8]) but we did not observe this increase in our tissue measurements. We will consider the area of the lamina propria to be the same for healthy subjects and patients with COPD. We now fix some notations.

Notation 2.1
1. *For any site $(i,j) \in \mathcal{L}$, $M(i,j)$ is the neighbourhood of (i,j), it is the set of $(i-1,j-1), (i-1,j), (i-1,j+1), (i,j-1), (i,j+1), (i+1,j-1), (i+1,j), (i+1,j+1)$ belonging to $\mathcal{L}$. For a site inside the lamina propria the cardinal of $M(i,j)$ is 8 and lower if this site is at the edge of $\mathcal{L}$. We will note in the following $|M(i,j)|$ the number of elements of $M(i,j)$. In the literature, Moore's neighbourhood is $M(i,j) \cup \{(i,j)\}$.*
2. *A site of $\mathcal{L}$ has the code 1 (resp. 2) if it contains a F (resp. C) cell . If the site is empty it will be coded 0.*
3. *A configuration is an element $x = \big(x(i,j)\big)_{(i,j)\in\mathcal{L}}$ where $x(i,j)$ belongs to $\{0,1,2\}$ and $x(i,j) = 1$ (resp. $x(i,j) = 2$) means that a F (resp. C) cell occupies the site (i,j) and $x(i,j) = 0$ when the site (i,j) is empty. The set of configurations is $\{0,1,2\}^{\mathcal{L}}$ and is identified with $\{0,1,2\}^{|\mathcal{L}|}$.*
4. *For any $s = (i,j)$, $V(F)(s)$ (resp. $V(C)(s)$) denotes the number of F (resp. C) cells near s*

$$V(F)(s) = \sum_{s'\in M(s)} 1_{\{x(s')=1\}}, \quad V(C)(s) = \sum_{s'\in M(s)} 1_{\{x(s')=2\}}.$$

$V(s)$ is the number of F and C cells close to s :

$$V(s) = V(F)(s) + V(C)(s) = \sum_{s'\in M(s)} 1_{\{x(s')=1 \text{ or } 2\}} = \sum_{s'\in M(s)} 1_{\{x(s')\neq 0\}}.$$

2.1.2 Cell death

We suppose that a F cell has a probability p_{dF} of dying.
We define for each C cell a "basal" probability p_{dC} of dying, and an increased probability p_{dC+} of dying when the C cell has many other C cells in its neighbourhood. We distinguish two cases :

1. if C cell has few C neighbours ($V(C)(s) < \sigma$, where σ is an unknown integer), then this C cell attemps to die with the probability p_{dC}
2. If C cell has many C neighbours ($V(C)(s) \geq \sigma$), then C cell attemps to die with the probability p_{dC+}.

The introduction of the probability p_{dC+} is justified by a recent study ([27]) showing the existence of CD8+ T cell-population-intrinsic mechanisms regulating cellular behavior, with induction of apoptosis to avoid an excessive increase in T cell population.
The numerical values of p_{dC}, p_{dC+}, σ and p_{dF} will be presented in Section 3.1.2.

2.1.3 Proliferation of C cell

We recall that a F cell does not proliferate, so we will take $p_F = 0$. Consider a C cell located in s.

1. If all sites in $M(s)$ are occupied (i.e. $V(s) = |M(s)|$), or if all empty s' sites belonging to $M(s)$ have "many" C neighbours (i.e. $V(C)(s') \geq \lambda$, where λ is an integer to be specified), the C cell does not divide.
2. There exists at least one empty site $s' \in M(s)$ such that $V(C)(s') < \lambda$.
   (a) If there is no F cell in $M(s)$, the C cell attempts to divide with the probability p_C.
   (b) If there is at least one F cell in $M(s)$, the C cell attempts to divide with the probability $p_{C/F}$.

   If proliferation occurs, we decide that C remains in s and we uniformly choose an unoccupied site s' belonging to $M(s)$, such that $V(C)(s') < \lambda$, on which we create a new cell.

Since in the absence of stimulation, the major part of C cells do not divide in the lung ([10]), we will therefore consider that in the absence of any other stimulation, the probability p_C that a C cell divide in the peribronchial area is zero, for control subjects as well as COPD patients :

$$p_C^{ctl} = p_C^{COPD} = 0. \tag{2.1}$$

Previous studies indicate that the doubling time of C cells *in vivo* after a stimulation such as a contact with a fibrocyte is estimated around $4h$ ([26], [14]). We will consider an average duration of $4h = 80 \times 3min$ for a cell cycle of a C cell when a F cell is in its close environment. For healthy subjects, the increased probability $p_{C/F}$ of dividing will therefore be taken equal to 1/80. This probability is identical for control subjects and COPD patients :

$$p_{C/F}^{ctl} = p_{C/F}^{COPD} = 1/80 = 1.25 \times 10^{-2}. \tag{2.2}$$

2.1.4 Displacement of C and F cells

Let $s = (i, j)$ and $s' = (i', j')$ be two sites of the lamina propria. A cell can only move to a site adjacent to the occupied site :

$$P_F(s, s') = P_C(s, s') = 0 \text{ if } s' \notin M(s) \cup \{s\} \text{ or } s' \in M(s) \text{ and is occupied}$$

where $P_F(s, s')$ (resp. $P_C(s, s')$) denotes the probability that a F (resp. C) cell has to move from s to s'.

Our chemotaxis experiments show that F cells are significantly attracted towards the secretion of C cells, whatever the condition of the subject (control or COPD). This leads us to take

$$P_F(s,s') = \begin{cases} k_F f_F\big(V(C)(s')\big) & \text{if } s' \in M(s) \text{ and } s' \text{ is empty} \\ k_F x_F & \text{if } s' = s \end{cases} \tag{2.3}$$

where $x_F > 0$, f_F is a function defined on $\{0,1,2,\cdots,8\}$ taking positive values and

$$k_F = \frac{1}{x_F + \sum_{s' \in M(s)} f_F\big(V(C)(s')\big) 1_{\{s' empty\}}}. \tag{2.4}$$

Since this chemotactic effect requires soluble factors that have to be secreted in a sufficient concentration, this justifies an almost zero attraction ($\epsilon_F > 0$ "small", arbitrarily chosen as $\epsilon_F = 10^{-3}$) for s' such as $V(C)(s') < 3$ cells and a maximal and constant attraction for s' such as $V(C)(s') = 3$ or 4 cells. On the other hand, the attraction of the site s' for a F cell probably decreases when the site is too "crowded", because of physical hindrance and/or the secretion of factors that are secreted when many C cells are aggregated. For control subjects, we have thus chosen $f_F^{ctl}(n) = 1$ (resp. $f_F^{ctl}(n) = \epsilon_F$) if $n \in \{3,4\}$ (resp. $n \in \{0,1,2,5,6,7,8\}$). Our chemotaxis experiments show that secretions from C cells isolated from parenchyma of COPD patients are more attractive for F cells than those of C cells isolated from control patients, indicating that a smaller number of C cells is required to attract F cells in pathological condition than in healthy situation. For patients with COPD, we have thus chosen : $f_F^{COPD}(n) = 1$ (resp. $f_F^{COPD}(n) = \epsilon_F$) if $n \in \{2,3,4\}$ (resp. $n \in \{0,1,5,6,7,8\}$).
We now consider the case of a C cell alive and occupying the site s. It will move to the site $s' \in M(s) \cup \{s\}$, with probability

$$P_C(s,s') = \begin{cases} k_C f_C\big(V(s')\big) & \text{if } s' \in M(s), s' \text{ is empty} \\ k_C x_C & \text{if } s' = s \end{cases} \tag{2.5}$$

with $x_C > 0$, f_C is a function defined on $\{0,1,2,\cdots,8\}$ taking positive values and

$$k_C = \frac{1}{x_C + \sum_{s' \in M(s)} f_C\big(V(s')\big) 1_{\{s' empty\}}}. \tag{2.6}$$

Based on the same type of justifications than those used for F cells, f_C^{ctl} is the function defined on $\{0,1,2,5,6,7,8\}$ such that $f_C^{ctl}(n) = 1$ (resp. $f_C^{ctl}(n) = \epsilon_C$ where $\epsilon_C = 10^{-3}$) if $n \in \{4,5\}$ (resp. $n \in \{0,1,2,3,6,7,8\}$). We will consider that f_C is identical in control subjects and COPD patients, leading to $f_C^{ctl} = f_C^{COPD}$.
The values of x_F and x_C will be determined in Section 3.1.3.

2.1.5 Infiltration of C and F cells at the stable state

For F and C cells, there is an infiltration phenomenon at the stable state, which is amplified during exacerbations. We will add at the beginning of each $3mn$ time step, one F (resp. C) cell with probability p_{istaF} (resp. p_{istaC}) to take into account the phenomenon of infiltration during the stable state. These probabilities will be determined from biological considerations (see Section 3.1.4). The choice of the value of $3mn$ will be justified later in Section 2.1.7. If a cell is recruited, we randomly and uniformly position it among the empty sites adjacent to the cell considered. If there are no empty sites nearby, no cell is added.

2.1.6 Infiltration of F and C cells during exacerbations

For a healthy subject, there is no exacerbation. According to [4], in COPD patients, there is an increase in the concentration of F cells in the blood during exacerbations. In the lungs, the density of F cells is higher in tissues of COPD patients than in those of healthy subjects ([5]), suggesting that for COPD patients, F cells are recruited from the blood to the lungs at the time of exacerbations. To take into account the excess of F cells infiltration during this particular event, we will add, each year, a number $N(iexaF)$ of F cells, with the probability p_{iexaF} so that after 20 years, on average, the number of F cells in COPD patients is double than in healthy patients. If cells are added, they are placed uniformly on the empty sites of the lamina propria.
The relationships between C cell infiltration and exacerbation are not entirely clear. For simplification, we will assume that there is no C cell infiltration during exacerbations. Thus, for a healthy subject as well as for a patient with COPD the value of p_{iexaC} is zero.

2.1.7 The different time scales

According to [18] the median speed of a C cell measured in lung tissue during 15 minutes is

$$v_0 = 2.3\ \mu m/mn. \tag{2.7}$$

Since we have no information on the *in vivo* speed of a F cell, we will assume that its speed is identical to that of a C cell. For an idealized cell modeled by a square with a side length $x_0 = 7\ \mu m$, v_0 thus represents approximately a movement of one square (lattice site) every $t_0 = 3$ minutes. We therefore set the duration of a time step to 3 min.
The time steps are denoted k, where $1 \leq k \leq T$ and T is of the order $3\ 504\ 000 = 20 \times 365 \times 24 \times 20$ (20 years, the order of magnitude of the time it takes between the beginning of cigarette smoke exposure and the onset of the disease). To take into account cell death, proliferation, displacement, duplication of cells we use the procedure given in Section 2.1.8 : we divide each time step k in N_k sub-time steps, where N_k is the number of cells at the beginning of time step k. At each sub-time step, a cell is drawn at random and can die, proliferate or move. We will consider more finely that v_0 is a median in Proposition 3.2.

2.1.8 The dynamics of C and F cells

Let us consider the beginning of the time step $k+1$. There are $N_k(F)$ F cells and $N_k(C)$ C cells, then $N_k = N_k(C) + N_k(F)$. If a C or F cell is added by infiltration at the stable state (cf subsection 2.1.5) we consider however that it is not part of the N_k initial cells, and cannot be drawn at random afterwards. It is therefore neither subject to death, nor to proliferation, nor to displacement during the time step $k+1$, it is just considered as present.
We divide the time step $k+1$ into N_k sub-time steps. For each sub-time step, we randomly draw a cell among the N_k present (with the probability $1/N_k$). Several cases can occur.

1. If the selected cell is dead or if it is a C cell that gave birth to a new cell by proliferation in a previous sub-time step, nothing happens.
2. Assuming in the following that the selected cell is alive and is not a "mother" cell, we denote by (i, j) the site occupied by this cell. The cell attempts to die following the procedure described in Subsection 2.1.2.

3. Suppose that the randomly drawn cell does not die.
   (a) If the selected cell is F, it moves according to the rule described in Section 2.1.4.
   (b) If it is a C cell,
      i. it divides according to the procedure described in Section 2.1.3. If the cell proliferates, we consider that the cell that has been added is not part of the population of N_k cells ;
      ii. otherwise, it moves according to the rule described in Section 2.1.4.

When the N_k subtime steps have been repeated independently we add to the initial population cells that are either born by proliferation or recruited by infiltration. Dead cells are removed. The number of cells is then N_{k+1}. We start a new cycle of N_{k+1} sub-time steps, as previously described. Therefore, over a time step, a given cell will on average die, move or divide (if it is a C cell).
Infiltration during exacerbation : Every year, i.e. after 175 200 time steps, we add a number $N(iexaF)$ of F cells with the probability p_{iexaF}. If F cells are recruited by infiltration during an exacerbation, they are randomly and uniformly positioned among all of the vacant sites. Cells that have infiltrated in the meantime are added to the initial population. A new time step starts again as described above.

2.2 Markov property

We start by setting some notations.

Definition 2.2 *1. For any k belonging to $\{1, \cdots, T\}$, $X_k = \big(X_k(i,j)\big)_{(i,j)\in\mathcal{L}}$ represents the state of the lamina propria at the end of the k time step. According to item 3 of Notation 2.1, $X_k(i,j) = 1$ (resp. $X_k(i,j) = 2$) means that a F (resp. C) cell occupies the site (i,j) and $X_k(i,j) = 0$ when the site (i,j) is empty. X_k is a random variable which takes its values in $\{0,1,2\}^{\mathcal{L}}$.*

2. ν_0 is the distribution of the initial state X_0, its value will be given in Section 3.1.1

3. Let $N_k(C)$ (resp. $N_k(F)$) be the number of C (resp. F) cells at the end of time step k.

We adopt the notations used in the theory of random processes : for any initial probability μ on $\{0,1,2\}^{\mathcal{L}}$, $\mathbb{P}_\mu$ represents the probability under which the law of X_0 is μ.

Proposition 2.3 *$(X_k)_{k\geq 0}$ is a recurrent, irreducible, a-periodic Markov chain that admits an unique invariant probability ν.*

Proof. Note that

$$N_k(F) = \sum_{(i,j)\in\mathcal{L}} 1_{\{X_k(i,j)=1\}}, \quad N_k(C) = \sum_{(i,j)\in\mathcal{L}} 1_{\{X_k(i,j)=2\}}.$$

Therefore, if $x = X_k$ is known, the quantities $N_k(F)$ and $N_k(C)$ are fixed, as well as the composition of each neighbourhood. It is then possible to write $X_{k+1} = F(X_k, \xi)$, where F is a function and $\xi = (\xi_i)_{i\geq 1}$ is a sequence of independent random variables and with uniform law on $[0,1]$, independent of X_k. The Markovian property is immediately deduced from this. It is straighforward to prove that the Markov chain is recurrent and irreducible. Since $\mathbb{P}_x(X_1 = x) > 0$, for any x, it is a-periodic. Therefore $(X_k)_{k\geq 0}$ admits a unique invariant probability. ■

To obtain the equilibrium state during simulations, one could think of using the Prott algorithm which allows to carry out exact simulations, see the seminal paper [19]. The lamina propria has a finite number of sites but too many (3 652), this algorithm only works when a "sandwiching" hypothesis is realized, see Chap. 11 in [7]. Unfortunately, in our context this assumption is not satisfied.

Corollary 2.4 *Let μ be an initial law on $\{0,1,2\}^{\mathcal{L}}$. The two sequences of random variables $\big(N_k(F)\big)_{k\geq 0}$ and $\big(N_k(F)\big)_{k\geq 0}$ converge in law when k tends to infinity. Moreover there is convergence of the means :*

$$\lim_{k\to\infty} \mathbb{E}_\mu\big(N_k(F)\big) = \mathbb{E}_\nu\big(N_0(F)\big), \quad \lim_{k\to\infty} \mathbb{E}_\mu\big(N_k(C)\big) = \mathbb{E}_\nu\big(N_0(C)\big).$$

Proof. We only deal with F cells. Note that $\mathbb{P}_\mu\big(N_k(F)=l\big) = \mathbb{P}_\mu\big(X_k \in A(l,F)\big)$, where l is an integer and $A(l,F) = \Big\{x,\ \sharp\big\{(i,j)\in\mathcal{L}, \text{ such that } x(i,j)=1\big\} = l\Big\}$. We deduce the convergence in law of $N_k(F)$, as $k\to+\infty$. Moreover :

$$\begin{aligned}\lim_{k\to\infty} \mathbb{E}_\mu\big(N_k(F)\big) &= \lim_{k\to\infty} \Big(\sum_{l=0}^{|\mathcal{L}|} l\ \mathbb{P}_\mu\big(X_k\in A(l,F)\big)\Big)\\ &= \sum_{l=0}^{|\mathcal{L}|} l\ \mathbb{P}_\nu\big(X_k\in A(l,F)\big) = \mathbb{E}_\nu\big(N_k(F)\big) = \mathbb{E}_\nu\big(N_0(F)\big).\end{aligned}$$

■

2.3 The toy model

The toy model is a special case of the interaction model with the parameters

$$\sigma = 9, \quad p_C = 0, \quad \lambda = 0. \tag{2.8}$$

This means that C and F cell displacement, the stable infiltration and that due to exacerbations (see Section 2.1.5, resp. 2.1.6) are identical to those in the complete model. However, C cells do not proliferate at all (i.e. $p_C = 0$ and $\lambda = 0$) and die with the probability p_{dC} independently of the local context ($\sigma = 9$).
Since the toy model is a special case of the interaction model, the results of Section 2.2 apply. In particular, the toy model is Markovian.

3 Results

3.1 Determination of parameters via biological information

We will use the toy model for which a probabilistic analysis is possible to determine numerical values for the parameters ν_0, p_{dC}, p_{dF}, x_C, x_F, p_{istaC}, p_{istaF} p_{iexaF} and $N(iexaF)$ for healthy subjects and patients with COPD. We will proceed in two steps. For each parameter considered, we will start by stating a mathematical property formulated in the framework of the mathematical toy model. Then, the use of biological data will allow to deduce a numerical value of the parameter which will be used for the simulations. For ease of reading, the proofs are pushed back to Section 5.

3.1.1 The initial cell distribution

For the initial distribution ν_0, we first used the mean of the densities of C and F cells measured on tissues from non-smokers subjects, reflecting the "healthy" situation : $DENS_0(C) = 0.660 \times 10^{-3}$ cells/μm^2 and $DENS_0(F) = 0.106 \times 10^{-3}$ cells/μm^2. To obtain these densities with a lattice of 3652 sites (*i.e.* 178 948μm^2), we will therefore consider

$$\begin{array}{rcl} N_0(C) & = & n_0(C) = 0.660 \times 10^{-3} \times 179\,000 \approx 118 \\ N_0(F) & = & n_0(F) = 0.106 \times 10^{-3} \times 179\,000 \approx 19. \end{array} \tag{3.1}$$

Second we choose the $n_0(C)$ (resp. $n_0(F)$) C (resp. F) cells uniformly distributed in the lamina propria. Random spatial representations can be obtained with determinantal point processes. We have not retained them because they rather model repulsive phenomenons and therefore they are not adapted to our interaction model. Moreover their simulation is delicate, see [13].

3.1.2 Determination of p_{dC} and p_{dF}

We take into account that, for a healthy subject, the half-lives $hl(C)$ and $hl(F)$ of C and F cells are known. We consider a F cell at time 0 or a C cell at time 0 or just born. Let us note $T(C)$ (resp. $T(F)$) the life time of a C (resp. F) cell and $q_{1/2}\big(T(C)\big)$ (resp. $q_{1/2}\big(T(F)\big)$) its median. Recall that the median of a probability law is its quantile of order 1/2.

Proposition 3.1 *We have*

$$\Big\lfloor \frac{\ln 2}{\ln\big\{1/(1-p_{dC})\big\}} \Big\rfloor \;\leq\; q_{1/2}\big(T(C)\big) \leq 1 + \frac{\ln 2}{2(1-p_{dC})^2} + \Big\lfloor \frac{\ln 2}{\ln\big\{1/(1-p_{dC})\big\}} \Big\rfloor \tag{3.2}$$

$$\Big\lfloor \frac{\ln 2}{\ln\big\{1/(1-p_{dF})\big\}} \Big\rfloor \;\leq\; q_{1/2}\big(T(F)\big) \leq 1 + \frac{\ln 2}{2(1-p_{dF})^2} + \Big\lfloor \frac{\ln 2}{\ln\big\{1/(1-p_{dF})\big\}} \Big\rfloor \tag{3.3}$$

where $\lfloor x \rfloor$ is the greatest integer less than or equal to x.

It is known from the literature ([17] and [22]) that

$$hl^{ctl}(C) = 14 \text{ days } = 6\,720 \text{ time steps}, \quad hl^{ctl}(F) = 10 \text{ months } = 144\,000 \text{ time steps}. \tag{3.4}$$

We choose $hl^{ctl}(C) = \frac{\ln 2}{\ln\left\{1/(1-p_{dC})\right\}}$ (resp. $hl^{ctl}(F) = \frac{\ln 2}{\ln\left\{1/(1-p_{dF})\right\}}$), i.e.

$$p_{dC}^{ctl} = 1 - e^{-\ln 2/hl^{ctl}(C)} \approx 1.0 \times 10^{-4}, \quad p_{dF}^{ctl} = 1 - e^{-\ln 2/hl^{ctl}(F)} \approx 4.8 \times 10^{-6}. \tag{3.5}$$

Therefore $\frac{\ln 2}{2(1-p_{dC}^{ctl})^2} \approx 0.151$ and $\frac{\ln 2}{2(1-p_{dF}^{ctl})^2} \approx 0.151$. Inequalities (3.2) and (3.3) imply that the median of $T(C)$ (resp. $T(F)$) is reasonably close to $hl^{ctl}(C)$ (resp. $hl^{ctl}(F)$).
A study [24] suggests a modification of the C cell death processes in tissues from patients with COPD, with a decrease by about half of the percentage of apoptotic C cells in the distal airways of mild to moderate COPD patients, which constitute the majority of our study cohort. In patients with COPD, we will therefore choose for each C cell the probability p_{dC}^{COPD} of dying equal to

$$p_{dC}^{COPD} = p_{dC}^{ctl}/2 \approx 5 \times 10^{-5}. \tag{3.6}$$

Our previous work [5] showed that the exposure of fibrocytes to the secretions of the bronchial epithelia from patients with COPD decreases by a factor 2 the percentage of dead cells . Therefore we choose :

$$p_{dF}^{COPD} = p_{dF}^{ctl}/2 \approx 2.4 \times 10^{-6}. \tag{3.7}$$

Our measurements performed in lung tissues showed that clusters of C cells contain a median value of approximately 4 cells. Thus, we choose $\sigma = 3$ neighbours, to favor cell death for a neighbourhood comprising 3 or more C neighbours. This value is unchanged in patients with COPD vs control subjects :

$$\sigma^{ctl} = \sigma^{COPD} = 3. \tag{3.8}$$

Studies show that lymphocyte cell death is increased by a factor 4 in a crowed environment ([21], [27]). We therefore choose : $p_{dC+} = 4p_{dC}$. We thus obtain :

$$p_{dC+}^{ctl} = 4p_{dC}^{ctl} \approx 4.0 \times 10^{-4}, \quad p_{dC+}^{COPD} = 4p_{dC}^{COPD} \approx 2.0 \times 10^{-4}. \tag{3.9}$$

3.1.3 Determination of x_C and x_F

Since C and F cells behave in a similar way, we will detail the following analysis only for F cells. Let $\alpha > 0$ be a real number such that

$$\mathbb{P}(Y_\alpha \leq 4) = \frac{1}{2}, \quad \text{where } Y_\alpha \sim \mathcal{P}(\alpha). \tag{3.10}$$

It is easy to determine numerically the value of α, we find $\alpha \approx 4.67091$.
Consider a F cell occupying the site s and which is alive and not completely surrounded. According to (2.3), F moves with probability $p_{moveF} = 1 - k_F x_F$. Since $\alpha < 5$, we can easily deduce from relation (2.4) that there is a unique x_F such that

$$p_{moveF} = 1 - k_F x_F = \frac{\alpha}{5} \approx 0.9342. \tag{3.11}$$

This leads to :

$$x_F = \frac{1-\alpha/5}{\alpha/5}\Big(\sum_{s' \in M(s)} f_F\big(V(C)(s')\big)1_{\{s' empty\}}\Big),\ k_F = \frac{\alpha/5}{\sum_{s' \in M(s)} f_F\big(V(C)(s')\big)1_{\{s' empty\}}}. \tag{3.12}$$

During a subperiod, if F is chosen, does not die and is completely surrounded, it cannot move, but we agree that it can have a virtual move with probability $\alpha/5$. We note $Z_k(moveF)$ (resp. $Z'_k(moveF)$) the number of real (resp. real and virtual) moves during the time-step $k+1$. It is interesting to introduce the random variable $Z'_k(moveF)$ since its law under $\mathbb{P}_{\nu_0}^{|k}$ is $\mathcal{B}\Big(N_k, \frac{(1-p_{dF})\alpha}{5N_k}\Big)$, where

$$\mathbb{P}_{\nu_0}^{|k} \text{ is the conditional expectation given } X_k. \tag{3.13}$$

Proposition 3.2 *We have :*

$$\mathbb{P}_{\nu_0}^{|k}\big(Z_k(moveF) \neq Z'_k(moveF)\big) \leq \frac{1}{N_k}\mathbb{E}_{\nu_0}^{|k}\big(\Gamma_k(F)\big) \tag{3.14}$$

where Γ_k is the number of times F is fully surrounded during the time step $k+1$.

We took $k = 5$ years $= 876\ 000$ time periods, because we estimated that beyond this date the stationary state is reached. We considered an additional period and we performed 100 simulations of this scheme. For each simulation, $\Gamma_k(C) = \Gamma_k(F) = 0$ and the empirical mean of the $2/N_k$ is 0.015.
From (3.14) we deduce that the conditional law of the random variable $Z_k(moveF)$ is approximatively $\mathcal{B}\Big(N_k, \frac{(1-p_{dF})\alpha}{5N_k}\Big)$. The distance between the binomial law $\mathcal{B}(a,b)$ and the Poisson distribution $\mathcal{P}(ab)$ is lower than $\delta = 2\min(2, ab)b$ (see the Prohorov's inequality, section III.7 in [23]). In our case $\delta \leq 2/N_k$. Relations (3.5), (3.6) and (3.7) as well as our 100 simulations imply that the binomial distribution $\mathcal{B}\Big(N_k, \frac{(1-p_{dF})\alpha}{5N_k}\Big)$ can be accurately approximated by the Poisson distribution $\mathcal{P}(\alpha/5)$.
It is now possible to take into account the biological observation (2.7). During the $15\ mn = 5\times 3$ mn time intervals the F cell covers the distance of $x_0 Z$ μm where $Z = Z_k(moveF) + \cdots + Z_{k+4}(moveF)$ is the number of moves between the time steps $k+1$ and $k+5$ (recall from Section 2.1.1 that $x_0 = 7$ μm). It follows from above, that the law of Z is approximatively $\mathcal{P}(\alpha)$. The speed of F is thus $V(moveF) = \frac{x_0 Z}{15}$ $\mu m/mn$. Using (2.7) and (3.10) we get :

$$\mathbb{P}_{\nu_0}\big(V(moveF) \leq v_0\big) = \mathbb{P}_{\nu_0}(Z \leq 4.93) = \mathbb{P}_{\nu_0}\Big(Z_{move} \leq 4\Big) = \frac{1}{2}.$$

Remark 3.3 *For the C cells, there is a formula similar to* (3.14) *which is obtained by replacing the letter F by C. The real numbers x_C and k_C are given by*

$$x_C = \frac{1-\alpha/5}{\alpha/5}\Big(\sum_{s'\in M(s)} f_C\big(V(s')\big)1_{\{s' empty\}}\Big),\ k_C = \frac{\alpha/5}{\sum_{s'\in M(s)} f_C\big(V(s')\big)1_{\{s' empty\}}}. \quad (3.15)$$

3.1.4 Determination of p_{istaF} and p_{istaC}

Recall that according to Corollary 2.4, for k large enough

$$\mathbb{E}_{\nu_0}\big(N_k(C)\big) \approx \mathbb{E}_{\nu}\big(N_k(C)\big) = \mathbb{E}_{\nu}\big(N_0(C)\big), \quad \mathbb{E}_{\nu_0}\big(N_k(F)\big) \approx \mathbb{E}_{\nu}\big(N_k(F)\big) = \mathbb{E}_{\nu}\big(N_0(F)\big) \quad (3.16)$$

where ν is the invariant probability. However, the mean equilibrium values $\mathbb{E}_{\nu}\big(N_0(C)\big)$ and $\mathbb{E}_{\nu}\big(N_0(F)\big)$ are unknown.

Proposition 3.4 *We suppose that there is no infiltration during exacerbations, i.e. $N(iexaF) = p_{iexaF} = 0$. Then for any k we have :*

$$\mathbb{E}_{\nu_0}\big(N_k(C)\big) = \Big(n_0(C) - \frac{p_{istaC}}{p_{dC}}\Big)(1-p_{dC})^k + \frac{p_{istaC}}{p_{dC}} + \epsilon_k^C \quad (3.17)$$

$$\mathbb{E}_{\nu_0}\big(N_k(F)\big) = \Big(n_0(F) - \frac{p_{istaF}}{p_{dF}}\Big)(1-p_{dF})^k + \frac{p_{istaF}}{p_{dF}} + \epsilon_k^F \quad (3.18)$$

where ϵ_k^C and ϵ_k^F are positive numbers such that

$$\epsilon_k^C \leq \frac{p_{dC}}{2}\Big(\frac{p_{istaC}}{p_{dC}(1-p_{dC}/2)} + n_0(C)\Big), \quad \epsilon_k^F \leq \frac{p_{dF}}{2}\Big(\frac{p_{istaF}}{p_{dF}(1-p_{dF}/2)} + n_0(F)\Big). \quad (3.19)$$

Remark 3.5 *1. Since $\lim_{k\to\infty}(1-p_{dC})^k = 0$ (resp $\lim_{k\to\infty}(1-p_{dF})^k = 0$), then under the assumption that p_{dC} (resp. p_{dF}) is small, the general formula* (3.17) *(resp.* (3.18)*) implies*

$$\mathbb{E}_{\nu_0}\big(N_k(C)\big) \approx \frac{p_{istaC}}{p_{dC}}, \quad \Big(resp.\ \mathbb{E}_{\nu_0}\big(N_k(F)\big) \approx \frac{p_{istaF}}{p_{dF}}\Big) \quad for\ k\ large\ enough.$$

2. *For healthy patients, we want to determine the parameters p_{istaF} and p_{istaF} in such a way that $k \mapsto N_k(C)$ and $k \mapsto N_k(F)$ fluctuate little (at least at equilibrium) and remain close to $n_0(C)$ and $n_0(F)$ respectively. This leads us to take :*

$$p^{ctl}_{istaC} = p^{ctl}_{dC}\, n_0(C) = 1.18 \times 10^{-2}, \quad p^{ctl}_{istaF} = p^{ctl}_{dF}\, n_0(F) = 9.12 \times 10^{-5}. \tag{3.20}$$

We easily deduce that we have achieved our goal : $\mathbb{E}_{\nu_0}\big(N_k(C)\big) \approx n_0(C)$ and $\mathbb{E}_{\nu_0}\big(N_k(F)\big) \approx n_0(F)$, for k large enough.

3. *In pratice, in the COPD case, we choose to keep the relation $p^{COPD}_{istaC} = p^{COPD}_{dC}\, n_0(C)$ and as p_{dC} is different in patients with COPD than in healthy subjects (cf (3.6)), we obtain $p^{COPD}_{istaC} = p^{ctl}_{istaC}/2 = 5.9 \times 10^{-3}$.*
The case of F cells is analogous, we choose $p^{COPD}_{istaF} = p^{COPD}_{dF}\, n_0(F)$. Relation (3.7) leads to $p^{COPD}_{istaF} = p^{ctl}_{istaF}/2 = 4.56 \times 10^{-5}$.
Therefore the average number of C (resp. F) cells, not counting those added by exacerbation, is close to $n_0(C)$ (resp. $n_0(F)$).

3.1.5 Determination of $N(iexaF)$ and p_{iexaF} for COPD patients

For simplification, we will assume that there is no C cell infiltration during exacerbations. Then $p_{iexaC} = 0$. Thus, for healthy subjects as well as for patients with COPD $p^{ctl}_{iexaC} = p^{COPD}_{iexaC} = 0$. Concerning F cells, the value of p_{iexaF} depends closely on the condition of the subject. For a healthy subject, as there is no exacerbation, this probability is zero : $p^{ctl}_{iexaF} = 0$. For patients with COPD, we add N_{iexaF} F cells with probability p_{iexaF} every year, which is the average exacerbation frequency of patients with COPD. We make the same assumption as for stable infiltration : if we add N_{iexaF} F cells at the beginning of a year, these cells are not active immediately and they have to wait for the next time step before being active. In agreement with *in situ* measurements ([5]) the average number of F, after T time steps (i.e. 20 years), must be twice the number of F cells for a healthy subject.
According to item 2 of Remark 3.5, for an healthy subject, the expected number of F cells is close to the initial number $n_0(F)$ of F cells. Therefore the goal is to determine p_{iexaF} and $N(iexaF)$ such that

$$\mathbb{E}_{\nu_0}\big(N_T(F)\big) = 2n_0(F). \tag{3.21}$$

Proposition 3.6 *We choose :*

$$N(iexaF) = \left\lfloor \frac{K_1}{K_2} \right\rfloor + 1 \tag{3.22}$$

and

$$p_{iexaF} = \frac{1}{N(iexaF)} \frac{K_1}{K_2} \tag{3.23}$$

where

$$K_1 = \big(1 - (1-p_{dF})^{T_y}\big)\Big(2n_0(F) - (1-p_{dF})^{T}\Big(n_0(F) - \frac{p_{istaF}}{p_{dF}}\Big) - \frac{p_{istaF}}{p_{dF}}\Big) \tag{3.24}$$

$$K_2 = (1-p_{dF})^{T_y-1}\big(1 - (1-p_{dF})^{T}\big). \tag{3.25}$$

and $T_y = 175\,200$ *is the number of time steps in a year. Then*

$$0 \leq \mathbb{E}_{\nu_0}\big(N_T(F)\big) - 2n_0(F) \leq R' \tag{3.26}$$

where

$$\begin{aligned} R' \;=\; & \frac{1}{1-(1-p_{dF})^{T_y}} \Bigg\{ \frac{p_{istaF}}{2(1-p_{dF}/2)} + \frac{p_{dF}}{2}\big(p_{istaF} + N(iexaF)p_{iexaF}\big) \\ & + \frac{p_{dF}(1+p_{dF})}{2} \Bigg[n_0(F) + \Big(\frac{p_{istaF}}{p_{dF}}\big(1-(1-p_{dF})^{T_y}\big) \\ & + (1-p_{dF})^{T_y-1} N(iexaF)p_{iexaF} + \frac{p_{istaF}}{2(1-p_{dF}/2)} \\ & + \frac{p_{dF}}{2}\big(p_{istaF} + N(iexaF)p_{iexaF}\big)\Big) \frac{1}{1-(1-p_{dF})^{T_y} - p_{dF}(1+p_{dF})/2} \Bigg] \Bigg\}. \end{aligned} \tag{3.27}$$

Remark 3.7 *1. $N(iexaF)$ is the smallest integer such that* (3.23) *holds.*

2. Suppose that $p_{istaF} = p_{dF}\; n_0(F)$, then

$$\frac{K_1}{K_2} = \frac{n_0(F)\big(1-(1-p_{dF})^{T_y}\big)}{(1-p_{dF})^{T_y-1}\big(1-(1-p_{dF})^{T}\big)}.$$

3. Suppose $p_{istaF}^{COPD} = 4.56 \times 10^{-5}$. Then $p_{istaF}^{COPD} = p_{dF}^{COPD}\; n_0(F)$ and

$$N(iexaF) = 10, \quad p_{iexaF} \approx 0.993, \quad R' \approx 4.3 \times 10^{-4}.$$

Consequently, the expected number of C cells for COPD patients is reasonably close to $n_0(F)$.

3.2 Elements of simulation

Figure 1 shows the simulation results of fibrocytes and $CD8+$ T cells behaviors within the peribronchial area during 20 years, for healthy subjects and patients with COPD, obtained with the toy model. Figure 1A represents snapshots of the peribronchial area with fibrocytes, and CD8+ T cells at the beginning and at the end of the simulations. The distributions of cells are non-uniform for healthy subjects as well as for COPD patients after 20 years (Figure 1A). This is also visible on the movies 1 and 2, showing that these particular spatial distributions are (i) dynamic and (ii) already observed 5 years after initiation. An increased density of F cells as well as clusters of cells seems to be present in the sick condition (Figure 1A and movie 2). The relative distribution of cells will be explored in future studies. Simulations allowed us to analyze the dynamics of cells over time. We represent in Figure 1B the fluctuations of $k \to \overline{N(C)}_k$, where $\overline{N(C)}_k$ is the empirical mean of the number of C cells for the month k. They are close to 118 in the healthy condition, which is equal to the initial number of initial cells ($N_0(C) = 118$) and corroborate the theoretical results, cf Remark 3.5. Similar findings are found in the COPD condition.

To characterize the importance of cell death and infiltration, we plotted the number of C cells (resp F cells) that have died (Figure 1C, 1G) or infiltrated (Figure 1D, 1H) for each month. In agreement with experimental findings ([24]) taken into account in our model, cf (3.6), the death of C cells is reduced by two in COPD compared to control situation (Figure 1C). In both situations, the infiltration of C cells compensates C cell death (Figure 1D-E). Furthermore, as expected, the number $\overline{N(F)}_k$ doubles after 20 years, from the control

(mean $\overline{N(F)} = 20$) to the COPD condition (mean $\overline{N(F)} = 40$) (Figure 1F). The change in $\overline{N(F)}_k$ in the COPD condition is mainly the consequence of the infiltration of F cells during exacerbations (Figure 1G-H), as shown by the cumulative numbers of F cells that have died and infiltrated (Figure 1I). This result was anticipated by our mathematical analysis, see Section 3.1.5, but the simulations allow us to show that the fluctuations are reasonable and seem to reproduce patients heterogeneity.

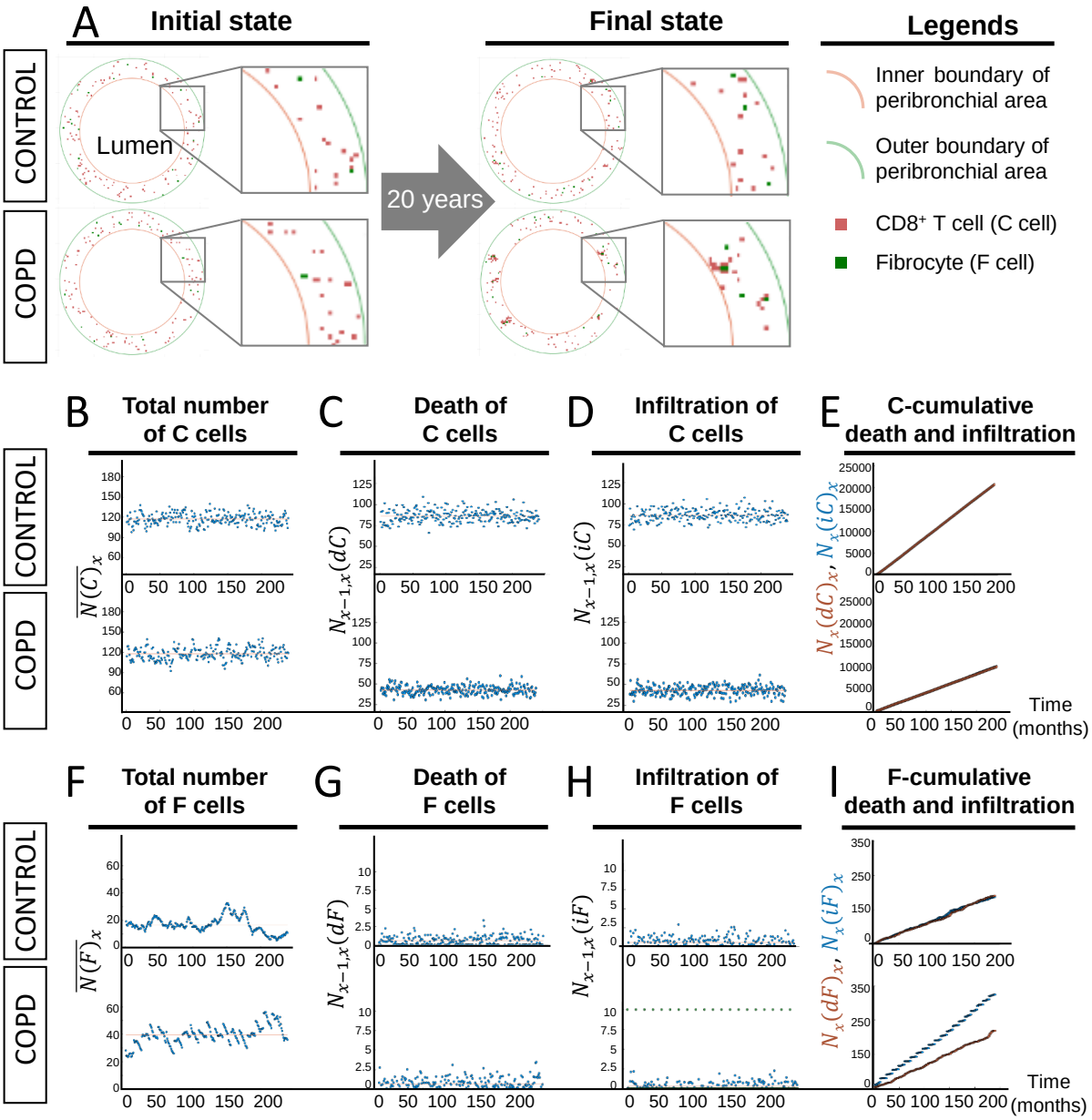

Figure 1. Simulation results of cell dynamics within the peribronchial area during 20 years, for healthy subjects and patients with COPD, obtained with the toy model. **A)** Selected representative pictures for control (top panels) and COPD (bottom panels) situations at initial state (left panels) and after 20 years (right panels). CD8+ T cells (C cells) and fibrocytes (F

cells) are represented respectively by pink and green squares. Panels surrounded by grey : higher magnifications of peribronchial area. **B, F)** Graphs showing the time variations of $x \to \overline{N(C)}_x$ in panel B (resp. $x \to \overline{N(F)}_x$ in panel F), where $\overline{N(C)}_x$ (resp. $\overline{N(F)}_x$) is the empirical mean of the number of C (resp. F) cells for the month x. The average of $N(C)_x$ and $N(F)_x$ over the 20 years-period are indicated by red lines. **C, G**) Graphs showing the variations of $N_{x-1,x}(dC)$ (panel C) and $N_{x-1,x}(dF)$ (panel G) over time. $N_{x-1,x}(dC)$ and $N_{x-1,x}(dF)$ are the number of C (resp. F) cells that have died for the month x. **D, H**) Graphs showing the variations of $N_{x-1,x}(iC)$ (panel D) and $N_{x-1,x}(iF)$ (panel H) over time. $N_{x-1,x}(iC)$ and $N_{x-1,x}(iF)$ are the number of C (resp. F) cells that have infiltrated the peribronchial area for the month x. The infiltration at the stable state and during exacerbation are indicated respectively in blue and green. For control situation, there is no infiltration by exacerbation. **E, I)** Cumulative distributions of the numbers of C cells $N_x(dC)$ and F cells $N_x(dF)$ that have died during the month x (red curve), and the numbers of C cells $N_x(iC)$ and F cells $N_x(iF)$ that have infiltrated the surface of interest during the month x (blue curve).

Movie legends
Cell dynamics within the peribronchial area, 5 years after the beginning the initial time, images of the simulations were recorded every 3 min during 24 hours. CD8+ T cells (C cells) and fibrocytes (F cells) are represented respectively by pink and green squares.
Movie 1 (resp. 2) : control (resp. COPD) situation.

4 Conclusion and discussion

In order to gain insights about the reasons for the breakdown of homeostasis that could emerge from slight deregulations of normal cellular processes in COPD, we developed a probabilistic cellular automaton mathematical model to replicate cell-scale properties of two different cell populations, fibrocytes and CD8+ T cells. It takes into account individual cell motility, death, proliferation and infiltration processes with rules that are dependent on the local microenvironment. We assume that the diseased and healthy states are obtained for two distinct sets of parameters. We have introduced a simpler model in which one can mathematically compute probabilities of events or expectations of random variables of interest. This allowed to accurately derive the parameters according to biologically observations in human tissues and *in vitro* experiments. The results from the simulations suggest that modifications of the parameters are sufficient to generate an increased density of fibrocytes in the COPD situation compared to the healthy one, as well as different spatial distributions, which are consistent with *in situ* observations. This has not been achieved using any experimental approaches previously.
Several assumptions were made to simplify this initial model. Parameters were estimated from biological data using the toy model, and their validity in the complete model is unknown. Our Markov model does not take into account memory effects, which could play a role in disease onset and evolution. In addition, cell interactions inside tissues are far more complex than those considered in this system. In particular, it does not take into account all the other cells, such as epithelial cells, smooth muscle cells and other immune cells. Long-range effects, such as the attractive effect of the bronchial epithelium at the lumen border could be included by assigning different displacement probabilities based on the distance to the inner edge of the grid. Nevertheless, our model seems to us to be a very good starting version that we may have to complicate.

This model does not only propose causal explanations for *in situ* observations, but we also anticipate it to be predictive. For example, it would be particularly useful to answer the following pertinent clinical questions : is it possible to return from a pathological to a healthy state without any intervention ? Would a treatment modifying the local intercellular interactions reverse the pathological state ? At what time should the treatment be applied to be effective ?

5 Proofs of technical points

5.1 Proof of Proposition 3.1

Since the cells C and F play symmetrical roles, it is sufficient to consider a fixed C cell. We start with two preliminary lemmas 5.1 and 5.3.

Lemma 5.1 *Let $D_k(C)$ be the event "C dies during N_k sub-time steps of the time step $k+1$". Then*

$$P_{\nu_0}^{|k}\big(D_k(C)\big) = 1 - \Big(1 - \frac{p_{dC}}{N_k}\Big)^{N_k}. \tag{5.1}$$

and

$$p_{dC} - \frac{p_{dC}^2}{2} \leq P_{\nu_0}^{|k}\big(D_k(C)\big) \leq p_{dC}. \tag{5.2}$$

where $P_{\nu_0}^{|k}$ has been defined by (3.13).

Proof. To simplify the notations we denote by $\mathbb{P} = P_{\nu_0}^{|k}$. Let B_j be the event : "C is alive and does not die at the sub-time step j", $1 \leq j \leq N_k$. Then,

$$\mathbb{P}\big(B_j \big| B_1 \cap \cdots \cap B_{j-1}\big) = \frac{N_k - 1}{N_k} + \frac{1}{N_k}(1 - p_{dC}) = 1 - \frac{p_{dC}}{N_k}.$$

Reasoning by induction on j, we get :

$$\mathbb{P}\big(B_1 \cap \cdots \cap B_j\big) = \Big(1 - \frac{p_{dC}}{N_k}\Big)^j, \quad 1 \leq j \leq N_k. \tag{5.3}$$

Since $\overline{D_k(C)} = B_1 \cap \cdots \cap B_{N_k}$, then (5.1) follows. Inequality (5.2) is a consequence of

$$1 - \alpha x \leq (1-x)^\alpha \leq 1 - \alpha x + \frac{\alpha(\alpha-1)}{2}x^2, \quad 0 \leq x \leq 1,\ \alpha \geq 1. \tag{5.4}$$

■

Remark 5.2 *For a F cell, it is enough to change p_{dC} into p_{dF} and $D_k(C)$ into $D_k(F)$ in the identities* (5.1) *and* (5.2).

The estimate provided by Lemma 5.1 will be used twice, in the proofs of Lemma 5.3 and Proposition 3.4 (see Section 5.3).
Consider a C cell which is born at time step $k_0 - 1$ and which starts to be active at time step k_0. Let $T(C)$ be the lifetime of this cell, it is the first integer $k \geq 1$ such that the C cell dies at the time step $k_0 - 1 + k$. By definition $T(C) \geq 1$. The distribution of this variable is unknown. However, thanks to (5.2), we can give an approximation of its distribution function.

Lemma 5.3 *For any integer $k \geq 0$,*

$$(1-p_{dC})^k \leq \mathbb{P}_{\nu_0}\big(T(C) > k\big) \leq \Big(1 - p_{dC} + \frac{p_{dC}^2}{2}\Big)^k \tag{5.5}$$

Proof. Set $n = k_0 - 1 + k$, then

$$\mathbb{P}_{\nu_0}^{|n}\big(T(C) > k+1\big) = 1_{\{T(C)>k\}}\Big(1 - \mathbb{P}_{\nu_0}^{|n}\big(D_n(C)\big)\Big), \quad k \geq 0.$$

We take the expectation, using (5.2) we get :

$$(1-p_{dC})\mathbb{P}_{\nu_0}\big(T(C) > k\big) \leq \mathbb{P}_{\nu_0}\big(T(C) > k+1\big) \leq \Big(1 - p_{dC} + \frac{p_{dC}^2}{2}\Big)\mathbb{P}_{\nu_0}\big(T(C) > k\big).$$

The double inequality (5.5) is obtained by reasoning by recurrence on the integer k. ■

Recall that the median of a random variable Y with integer values is its quantile of order $1/2$:

$$q_{1/2}(Y) = \max\Big\{k \geq 1,\ \mathbb{P}(Y \leq k) \leq \frac{1}{2}\Big\}.$$

Lemma 5.4 *Let $0 < a \leq b < 1$, and Y be a random variable which takes its values in $\{1, 2, \cdots\}$ and such that :*

$$(1-b)^k \leq \mathbb{P}(Y > k) \leq (1-a)^k, \quad \forall\, k \geq 0. \tag{5.6}$$

Then

$$\Big\lfloor \frac{\ln 2}{\ln(1/(1-b))} \Big\rfloor \leq q_{1/2}(Y) \leq \Big\lfloor \frac{\ln 2}{\ln(1/(1-a))} \Big\rfloor. \tag{5.7}$$

Proof. For any $0 < \rho < 1$, we have :

$$n \geq \Big\lfloor \frac{\ln 2}{\ln(1/\rho)} \Big\rfloor + 1 \ \Leftrightarrow\ \rho^n < \frac{1}{2}. \tag{5.8}$$

We take $\rho = 1 - a$ and $k = \Big\lfloor \frac{\ln 2}{\ln(1/\rho)} \Big\rfloor + 1$. Relations (5.6) and (5.8) imply

$$1 - \mathbb{P}(Y \leq k) = \mathbb{P}(Y > k) \leq \rho^k < \frac{1}{2} \ \Rightarrow\ \mathbb{P}(Y \leq k) > \frac{1}{2} \ \Rightarrow\ q_{1/2}(Y) < k.$$

Similarly, with $\rho = 1 - b$ et $k = \Big\lfloor \frac{\ln 2}{\ln(1/\rho)} \Big\rfloor$ we get :

$$1 - \mathbb{P}(Y \leq k) = \mathbb{P}(Y > k) \geq \rho^k \geq \frac{1}{2} \ \Rightarrow\ \mathbb{P}(Y \leq k) \leq \frac{1}{2} \ \Rightarrow\ k \leq q_{1/2}(Y).$$

■

We now have all the elements to prove Proposition 3.1. We consider the relation (3.2) which only concerns the C cells. A direct use of inequalities (5.5) and (5.7) leads to : $q_- \leq q_{1/2}\big(T(C)\big) \leq q_+$, where :

$$q_- = \Big\lfloor \frac{\ln 2}{\ln\big\{1/(1-p_{dC})\big\}} \Big\rfloor, \quad q_+ = \Big\lfloor \frac{\ln 2}{\ln\Big\{1/\big(1-p_{dC}+\frac{p_{dC}^2}{2}\big)\Big\}} \Big\rfloor.$$

By an easy calculation, we have :

$$q_+ - q_- \leq 1 + \frac{\ln 2}{\ln\Big(1-p_{dC}+\frac{p_{dC}^2}{2}\Big)\ \ln(1-p_{dC})} \ln\Big(1+\frac{p_{dC}^2}{2(1-p_{dC})}\Big).$$

To obtain (3.2), it is enough to use $\ln(1+x) < x$, for any $x > -1$.

5.2 Proof of Proposition 3.2

If the F cell is never completely surrounded during time step $k+1$, then $Z_k(moveF) = Z'_k(moveF)$. Otherwise, let us note $i_1, \cdots, i_r$ the sub-periods when the F cell is fully surrounded where $r = \Gamma_k(F)$. Note that $Z_k(moveF) = Z'_k(moveF)$ means that there is no virtual move. Moreover the probability that a virtual shift occurs at time i_j is $\frac{1}{N_k}(1-p_{dF})\frac{\alpha}{5}$. Consequently

$$\mathbb{P}^{|k}_{\nu_0}\Big(Z_k(moveF) = Z'_k(moveF)\big|i_1, \cdots, i_r\Big) = \Big(1 - \frac{1}{N_k}(1-p_{dF})\frac{\alpha}{5}\Big)^{\Gamma_k(F)}.$$

Using (5.4) we have :

$$\mathbb{P}^{|k}_{\nu_0}\big(Z_k(moveF) < Z'_k(moveF)\big) \leq \frac{1}{N_k}(1-p_{dF})\frac{\alpha}{5}\ \mathbb{E}^{|k}_{\nu_0}\big(\Gamma_k(F)\big) \leq \frac{1}{N_k}\mathbb{E}^{|k}_{\nu_0}\big(\Gamma_k(F)\big).$$

5.3 Proof of Proposition 3.4

We start with a lemma which will also be used in the proof of Proposition 3.6.

Lemma 5.5 *Let $0 < \lambda < a < 1$, $\lambda_0 \geq 0$ and $b > 0$. We suppose that the two sequences of real numbers $(x_n)_{n\geq 0}$ and $(y_n)_{n\geq 1}$ satisfy*

$$x_{n+1} = (1-a)x_n + b + y_{n+1}, \quad n \geq 0 \tag{5.9}$$

with $x_0 \geq 0$ and

$$0 \leq y_{n+1} \leq \lambda_0 + \lambda x_n, \quad n \geq 0. \tag{5.10}$$

Then

$$x_n = \frac{b}{a}\big(1-(1-a)^n\big) + (1-a)^n x_0 + \epsilon_n, \quad n \geq 0 \tag{5.11}$$

where $\epsilon_0 = 0$ and for any $n \geq 1$,

$$0 \leq \epsilon_n \ \leq \ \frac{1}{a}\big(1-(1-a)^n\big)\left(\lambda_0 + \lambda\Big(\frac{b+\lambda_0}{a-\lambda} + x_0\Big)\right) \tag{5.12}$$

$$\leq \ \frac{1}{a}\left(\lambda_0 + \lambda\Big(\frac{b+\lambda_0}{a-\lambda} + x_0\Big)\right). \tag{5.13}$$

Proof. We deduce from (5.9) and (5.10) :

$$x_{n+1} \leq (1-a+\lambda)x_n + b + \lambda_0, \quad n \geq 0.$$

Note that $0 < 1-a+\lambda < 1$. A direct induction reasoning allows to show

$$0 \leq x_n \leq \frac{b+\lambda_0}{a-\lambda} + x_0, \quad n \geq 0. \tag{5.14}$$

We suppose that (5.11) occurs and show that this equality is verified when n is changed into $n+1$. Using both (5.9) and (5.10) we obtain :

$$x_{n+1} = \frac{b}{a}\big(1-(1-a)^{n+1}\big) + (1-a)^{n+1}x_0 + \epsilon_{n+1}$$

where $\epsilon_{n+1} = y_{n+1} + (1-a)\epsilon_n$. We set $\epsilon_0 = 0$, a reasoning by recurrence allows to show

$$\epsilon_{n+1} = (1-a)^{n+1}\Big(\sum_{k=0}^{n} \frac{y_{k+1}}{(1-a)^{k+1}}\Big), \quad n \geq 1.$$

Relations (5.10) and (5.14) imply :

$$\epsilon_{n+1} \leq \lambda_0\Big[\frac{1}{a}\big(1-(1-a)^{n+1}\big)\Big] + \lambda\Big[\Big(\frac{b+\lambda_0}{a-\lambda} + x_0\Big) \times \frac{1}{a}\big(1-(1-a)^{n+1}\big)\Big].$$

This shows (5.12) where n is changed into $n+1$. ■

We only prove(3.18). According to the definition of the toy model :

$$\mathbb{E}^{|k}_{\nu_0}\big(N_{k+1}(F)\big) = N_k(F) + p_{istaF} - N_k(F)P^{|k}_{\nu_0}\big(D_k(F)\big).$$

We take the expectation on both sides, we get

$$\mathbb{E}_{\nu_0}\big(N_{k+1}(F)\big) = (1-p_{dF})\,\mathbb{E}_{\nu_0}\big(N_k(F)\big) + p_{istaF} + \theta_{k+1} \tag{5.15}$$

where $\theta_{k+1} = \mathbb{E}_{\nu_0}\Big[\Big(p_{dF} - P^{|k}_{\nu_0}\big(D_k(F)\big)\Big)N_k(F)\Big]$. According to Lemma 5.1 :

$$0 \leq \theta_{k+1} \leq \frac{p^2_{dF}}{2}\mathbb{E}_{\nu_0}\big(N_k(F)\big).$$

Then applying Lemma 5.5 with $x_k = \mathbb{E}_{\nu_0}\big(N_k(F)\big)$ leads to

$$\mathbb{E}_{\nu_0}\big(N_k(F)\big) = \Big(n_0(F) - \frac{p_{istaF}}{p_{dF}}\Big)(1-p_{dF})^k + \frac{p_{istaF}}{p_{dF}} + \epsilon_k \tag{5.16}$$

and $0 \leq \epsilon_k \leq \frac{p_{dF}}{2}\Big(\frac{p_{istaF}}{p_{dF}(1-p_{dF}/2)} + n_0(F)\Big)$.

5.4 Proof of Proposition 3.6

The proof of Proposition 3.6 is based on the two lemmas 5.6 and 5.7.

Lemma 5.6 *For any* $0 \leq i \leq 19$ *:*

$$\begin{aligned}\mathbb{E}_{\nu_0}\big(N_{(i+1)T_y}(F)\big) &= (1-p_{dF})^{T_y}\,\mathbb{E}_{\nu_0}\big(N_{iT_y}(F)\big) + \frac{p_{istaF}}{p_{dF}}\big(1-(1-p_{dF})^{T_y}\big) \\ &\quad +(1-p_{dF})^{T_y-1}N(iexaF)p_{iexaF} + \eta_{i+1}\end{aligned} \tag{5.17}$$

and

$$0 \leq \eta_{i+1} \leq \frac{p_{istaF}}{2(1-p_{dF}/2)} + \frac{p_{dF}}{2}\big(p_{istaF}+N(iexaF)p_{iexaF}\big) + \frac{p_{dF}(1+p_{dF})}{2}\,\mathbb{E}_{\nu_0}\big(N_{iT_y}(F)\big) \tag{5.18}$$

where one year equals $T_y = 175\,200$ *time steps.*

Proof. **1)** Let $0 \leq i \leq 19$. We start from (5.15) and (5.16) and apply Lemma 5.5 with $x_k = \mathbb{E}_{\nu_0}\big(N_k(F)\big)$ where $iT_y + 1 \leq k \leq (i+1)T_y$:

$$\mathbb{E}_{\nu_0}\big(N_{(i+1)T_y}(F)\big) = \frac{p_{istaF}}{p_{dF}}\big(1-(1-p_{dF})^{T_y-1}\big) + (1-p_{dF})^{T_y-1}\mathbb{E}_{\nu_0}\big(N_{iT_y+1}(F)\big) + \epsilon_{T_y-1} \tag{5.19}$$

where

$$0 \leq \epsilon_{T_y-1} \leq \frac{p_{dF}}{2}\Big(\frac{p_{istaF}}{p_{dF}(1-p_{dF}/2)} + \mathbb{E}_{\nu_0}\big(N^{COPD}_{iT_y+1}(F)\big)\Big). \tag{5.20}$$

We add $N(iexaF)$ F cells with probability p_{iexaF}, at the end of the time step iT_y, reasoning as in the proof of Proposition 3.4, we have :

$$\mathbb{E}_{\nu_0}\big(N_{iT_y+1}(F)\big) = (1-p_{dF})\,\mathbb{E}_{\nu_0}\big(N_{iT_y}(F)\big) + p_{istaF} + N(iexaF)p_{iexaF} + \theta_1 \tag{5.21}$$

where

$$0 \leq \theta_1 \leq \frac{(p_{dF})^2}{2}\mathbb{E}_{\nu_0}\big(N_{iT_y}(F)\big). \tag{5.22}$$

Synthesizing (5.19) and (5.21) we obtain (5.17) and $0 \leq \eta_{i+1} = (1-p_{dF})^{T_y-1}\theta_1 + \epsilon_{T_y-1} \leq \theta_1 + \epsilon_{T_y-1}$.
Using (5.20), (5.21) and (5.22) we obtain :

$$\epsilon_{T_y-1} \leq \frac{p_{istaF}}{2(1-p_{dF}/2)} + \epsilon^*$$

where

$$\begin{aligned}\epsilon^* &= \frac{p_{dF}}{2}\Big[(1-p_{dF})\,\mathbb{E}_{\nu_0}\big(N_{iT_y}(F)\big) + p_{istaF} + N(iexaF)p_{iexaF} + \theta_1\Big] \\ &\leq \frac{p_{dF}}{2}\Big[p_{istaF} + N(iexaF)p_{iexaF}\big) + \mathbb{E}_{\nu_0}\big(N_{iT_y}(F)\big)\Big].\end{aligned}$$

Then inequality (5.18) follows directly. ■

Lemma 5.7 *We have :*

$$\begin{aligned}\mathbb{E}_{\nu_0}\big(N_T(F)\big) &= \frac{p_{istaF}}{p_{dF}} + (1-p_{dF})^T\Big(n_0(F) - \frac{p_{istaF}}{p_{dF}}\Big) \\ &\quad + \frac{(1-p_{dF})^{T_y-1}}{1-(1-p_{dF})^{T_y}}\big(1-(1-p_{dF})^T\big)N(iexaF)p_{iexaF}\Big) + \epsilon'_{20}\end{aligned} \tag{5.23}$$

where $0 \leq \epsilon'_{20} \leq R'$ *and* R' *has been defined by* (3.27).

Proof. We apply Lemme 5.5 with $x_i = \mathbb{E}_{\nu_0}\big(N_{iT_y}(F)\big)$ and $0 \leq i \leq 20$:

$$\begin{aligned}\mathbb{E}_{\nu_0}\big(N_T(F)\big) &= (1-p_{dF})^T\Big(n_0(F) - \frac{p_{istaF}}{p_{dF}} - \frac{(1-p_{dF})^{T_y-1}}{1-(1-p_{dF})^{T_y}}N(iexaF)p_{iexaF}\Big) \\ &\quad + \frac{p_{istaF}}{p_{dF}} + \frac{(1-p_{dF})^{T_y-1}}{1-(1-p_{dF})^{T_y}}N(iexaF)p_{iexaF} + \varepsilon'_{20}\end{aligned}$$

This shows (5.23). Moreover $0 \leq \varepsilon'_{20} \leq R'$. ■

We apply (5.23) and (3.23), we easily obtain :

$$\mathbb{E}_{\nu_0}\big(N_T(F)\big) = 2n_0(F) + \varepsilon'_{20}.$$

This implies (3.26).

References

[1] T. Afroj, A. Mitsuhashi, Ogino H., A. Saijo, K. Otsuka, H. Yoneda, M. Tobiume, N.T. Nguyen, H. Goto, K. Koyama, M. Sugimoto, O. Kondoh, H. Nokihara, and Y. Nishioka. Blockade of pd-1/pd-l1 pathway enhances the antigen-presenting capacity of fibrocytes. J. Immunol., 206(6) :1204–1214, 2021.

[2] L. Benítez, L. Barberis, and C.A. Condat. Modeling tumorspheres reveals cancer stem cell niche building and plasticity. Physica A : Statistical Mechanics and its Applications, 533 :121906, 2019.

[3] A. Deutsch and S. Dormann. Cellular automaton modeling of biological pattern formation. Modeling and Simulation in Science, Engineering and Technology. Birkhäuser/Springer, New York, 2017. Characterization, examples, and analysis, Second edition.

[4] I. Dupin, B. Allard, A. Ozier, E. Maurat, O. Ousova, E. Delbrel, T. Trian, H.-N. Bui, C. Dromer, O. Guisset, E. Blanchard, G. Hilbert, F. Vargas, M. Thumerel, R. Marthan, P.-O. Girodet, and P. Berger. Blood fibrocytes are recruited during acute exacerbations of chronic obstructive pulmonary disease through a cxcr4-dependent pathway. J. Allergy Clin. Immunol., 137 :1036–1042, 2016.

[5] I. Dupin, M. Thumerel, E. Maurat, F. Coste, E. Eyraud, H. Begueret, T. Trian, M. Montaudon, R. Marthan, P.-O. Girodet, and P. Berger. Fibrocyte accumulation in the airway walls of copd patients. Eur. Respir. J., 54, 2019.

[6] E. J. Hackett-Jones, K. A. Landman, D. F. Newgreen, and D. Zhang. On the role of differential adhesion in gangliogenesis in the enteric nervous system. J. Theor. Biol., 287 :148–159, 2011.

[7] O. Häggström. Finite Markov chains and algorithmic applications, volume 52 of London Mathematical Society Student Texts. Cambridge University Press, Cambridge, 2002.

[8] M. Hasegawa, Y. Nasuhara, Y. Onodera, H. Makita, K. Nagai, S. Fuke, Y. Ito, T. Betsuyaku, and M. Nishimura. Airflow limitation and airway dimensions in chronic obstructive pulmonary disease. Am. J. Respir. Crit. Care Med., 173 :1309–1315, 2006.

[9] H. Hatzikirou, L. Brusch, C. Schaller, M. Simon, and A. Deutsch. Prediction of traveling front behavior in a lattice-gas cellular automaton model for tumor invasion. Comput. Math. Appl., 59(7) :2326–2339, 2010.

[10] R.J. Hogan, L.S. Cauley, K.H. Ely, T. Cookenham, A.D. Roberts, J.W. Brennan, S. Monard, and D.L. Woodland. Long-term maintenance of virus-specific effector memory cd8+ t cells in the lung airways depends on proliferation. J. Immunol., 169 :4976–4981, 2002.

[11] J.C. Hogg, F. Chu, S. Utokaparch, R. Woods, W.M. Elliott, L. Buzatu, R.M. Cherniack, R.M. Rogers, F.C. Sciurba, H.O. Coxson, and P.D. Paré. The nature of small-airway obstruction in chronic obstructive pulmonary disease. N. Engl. J. Med., 350 :2645–2653, 2004.

[12] K. A. Landman and D. F. Newgreen. PCA modelling of multi-species cell clusters : ganglion development in the gastrointestinal nervous system. In Probabilistic cellular automata, volume 27 of Emerg. Complex. Comput., pages 261–277. Springer, Cham, 2018.

[13] C. Launay, B. Galerne, and A. Desolneux. Exact sampling of determinantal point processes without eigendecomposition. J. Appl. Probab., 57(4) :1198–1221, 2020.

[14] C.W. Lawrence and T.J. Braciale. Activation, differentiation, and migration of naive virus-specific cd8+ t cells during pulmonary influenza virus infection. J. Immunol., 173 :1209–1218, 2004.

[15] D. Lehotzky, R. Sipahi, and G. Zupanc. Cellular automata modeling suggests symmetric stem-cell division, cell death, and cell drift as key mechanisms driving adult spinal cord growth in teleost fish. Journal of Theoretical Biology, 509 :22, 2021.

[16] P.-Y. Louis and F. R. Nardi, editors. Probabilistic cellular automata. Theory, applications and future perspectives, volume 27. Springer, 2018.

[17] S.R. McMaster, J.J. Wilson, H. Wang, and J.E. Kohlmeier. Airway-resident memory cd8 t cells provide antigen-specific protection against respiratory virus challenge through rapid ifn-production. J. Immunol., 195 :203–209, 2015.

[18] P. Mrass, S.R. Oruganti, G.M. Fricke, J. Tafoya, J.R. Byrum, L. Yang, S.L. Hamilton, M.J. Miller, M.E. Moses, and J.L. Cannon. Rock regulates the intermittent mode of interstitial t cell migration in inflamed lungs. Nat. Commun., 2017.

[19] J. G. Propp and D. B. Wilson. Exact sampling with coupled Markov chains and applications to statistical mechanics. In Proceedings of the Seventh International Conference on Random Structures and Algorithms (Atlanta, GA, 1995), volume 9, pages 223–252, 1996.

[20] M. Saetta, A. Di Stephano, G. Turato, F.M. Facchini, L. Corbino, C.E. Mapp, P. Maestrelli, A. Ciaccia, and L.M. Fabbri. Cd8+ t-lymphocytes in peripheral airways of smokers with chronic obstructive pulmonary disease. Am. J. Respir. Crit. Care Med., 157 :822–826, 1998.

[21] P. Scheipers and H. Reiser. Fas-independent death of activated cd4+ t lymphocytes induced by ctla-4 crosslinking. Proc. Natl. Acad. Sci., 95 :10083–10088, 1998.

[22] J. Schyns, Q. Bai, C. Ruscitti, C. Radermecker, S. De Schepper, S. Chakarov, F. Farnir, D. Pirottin, F. Ginhoux, G. Boeckxstaens, F. Bureau, and T. Marichal. Non-classical tissue monocytes and two functionally distinct populations of interstitial macrophages populate the mouse lung. Nat. Commun., 10, 2019.

[23] A. N. Shiryayev. Probability, volume 95 of Graduate Texts in Mathematics. Springer-Verlag, New York, 1984. Translated from the Russian by R. P. Boas.

[24] L. Siena, M. Gjomarkaj, J. Elliot, E. Pace, A. Bruno, S. Baraldo, M. Saetta, M.R. Bonsignore, and A. Jame. Reduced apoptosis of cd8+ t-lymphocytes in the airways of smokers with mild/moderate copd. Respir. Med., 105 :1491–1500, 2011.

[25] H.S. Silva and M.L. Martins. A cellular automata model for cell differentiation. Physica A : Statistical Mechanics and its Applications, 322 :555–566, 2003.

[26] H. Yoon, T.S. Kim, and T.J. Braciale. The cell cycle time of cd8+ t cells responding in vivo is controlled by the type of antigenic stimulus. PLoS ONE, 5, 2010.

[27] S. Zenke, M.M. Palm, J. Braun, A. Gavrilov, P. Meiser, J.P. J.P. Böttcher, N. Beyersdorf, S. Ehl, A. Gerard, T. Lämmermann, T.N. Schumacher, J.B. Beltman, and J.C. Rohr. Quorum regulation via nested antagonistic feedback circuits mediated by the receptors cd28 and ctla-4 confers robustness to t cell population dynamics. Immunity, 52 :313–327, 2020.